Published December 6, 2004

Terminal osteoblast differentiation, mediated by runx2 and p27^{KIP1}, is disrupted in osteosarcoma

David M. Thomas,[1] Sandra A. Johnson,[4] Natalie A. Sims,[4] Melanie K. Trivett,[1] John L. Slavin,[1] Brian P. Rubin,[6] Paul Waring,[1] Grant A. McArthur,[1] Carl R. Walkley,[1] Andrew J. Holloway,[1] Dileepa Diyagama,[1] Jonathon E. Grim,[5] Bruce E. Clurman,[5] David D.L. Bowtell,[1] Jong-Seo Lee,[2] Gabriel M. Gutierrez,[2] Denise M. Piscopo,[2] Shannon A. Carty,[3] and Philip W. Hinds[2]

[1]Ian Potter Foundation Centre for Cancer Genomics and Predictive Medicine, and Sir Donald and Lady Trescowthick Laboratories, Peter MacCallum Cancer Center, Victoria 3002, Melbourne, Australia
[2]Department of Pathology, Harvard Medical School, Boston, MA 02115
[3]Albert Einstein College of Medicine of Yeshiva University, Bronx, NY 10461
[4]Department of Medicine, The University of Melbourne, St. Vincent's Hospital, Victoria 3065, Melbourne, Australia
[5]Divisions of Clinical Research and Human Biology, Fred Hutchinson Cancer Research Center, Seattle, WA 98109
[6]Department of Pathology, University of Washington, Seattle, WA 98195

The molecular basis for the inverse relationship between differentiation and tumorigenesis is unknown. The function of runx2, a master regulator of osteoblast differentiation belonging to the *runt* family of tumor suppressor genes, is consistently disrupted in osteosarcoma cell lines. Ectopic expression of runx2 induces p27^{KIP1}, thereby inhibiting the activity of S-phase cyclin complexes and leading to the dephosphorylation of the retinoblastoma tumor suppressor protein (pRb) and a G1 cell cycle arrest. Runx2 physically interacts with the hypophosphorylated form of pRb, a known coactivator of runx2, thereby completing a feed-forward loop in which progressive cell cycle exit promotes increased expression of the osteoblast phenotype. Loss of p27^{KIP1} perturbs transient and terminal cell cycle exit in osteoblasts. Consistent with the incompatibility of malignant transformation and permanent cell cycle exit, loss of p27^{KIP1} expression correlates with dedifferentiation in high-grade human osteosarcomas. Physiologic coupling of osteoblast differentiation to cell cycle withdrawal is mediated through runx2 and p27^{KIP1}, and these processes are disrupted in osteosarcoma.

Introduction

Osteosarcoma is the most common bone cancer in young adults, and a leading cause of cancer death in this age group. Loss of differentiation has powerful prognostic significance in osteosarcoma, with well-differentiated tumors being classified as low-grade and dedifferentiated tumors usually falling into the high-grade category. In one large series, 81% of osteosarcomas were either poorly differentiated or undifferentiated (Dahlin, 1957), and a late marker of osteogenic differentiation, osteocalcin, was undetectable in >75% of osteosarcomas (Hopyan et al., 1999). In vitro data support the view that osteoblast differentiation is antagonistic to oncogenic processes. Cellular immortalization attenuates expression of osteoblast phenotype (Bodine et al., 1996; Feuerbach et al., 1997), whereas osteoblast differentiation is associated with progressive loss of proliferative capacity, culminating in terminal cell cycle exit (Stein et al., 1996; Aubin, 1998). Although it is clear that differentiation is antithetical to tumor development in osteosarcoma, the molecular basis for the tightly coupled relationship between malignant transformation and loss of differentiation remains poorly understood.

The biology of osteoblast differentiation has recently been mapped in considerable detail. Runx2 (runt-related transcription factor 2) is a key transcriptional regulator of osteogenesis (Ogawa et al., 1993; Levanon et al., 1994; Ducy et al., 1997, 1999). Mice nullizygous for *RUNX2* exhibit a complete lack of ossification (Komori et al., 1997; Otto et al., 1997), whereas heterozygotes exhibit skeletal abnormalities comparable to cleidocranial dysplasia (Mundlos et al., 1997). The runt family, to which runx2 belongs, is strongly linked to human cancer (Lund and van Lohuizen, 2002). *RUNX1 (AML1)* is mutated in human leukemia, and mice expressing loss-of-function runx1 mutants are prone to leukemia (Perry et al., 2002). *RUNX3* is subject to inactivating mutations or promoter hypermethylation

Correspondence to David Thomas: david.thomas@petermac.org

G. Gutierrez's and P.W. Hinds's present address is Dept. of Radiation Oncology and Molecular Oncology Research Institute, Tufts-New England Medical Center, Boston, MA 02111.

Abbreviations used in this paper: BMP, bone morphogenetic protein; MEF, murine embryonic fibroblast; PCNA, proliferating cell nuclear antigen.

The Journal of Cell Biology, Vol. 167, No. 5, December 6, 2004 925–934
http://www.jcb.org/cgi/doi/10.1083/jcb.200409187

Published December 6, 2004

in gastric cancers (Li et al., 2002). Runx2 physically interacts with the retinoblastoma tumor suppressor protein (pRb; Thomas et al., 2001), which is mutated in up to 60% of osteosarcomas (Toguchida et al., 1989). Finally, runx2 expression varies with cell cycle status and may regulate osteoblast proliferation by unknown mechanisms (Pratap et al., 2003).

In this study, we investigated the effects of osteogenic differentiation on proliferation and growth arrest, and their disruption in osteosarcomas. Consistent with a role in suppression of proliferation, runx2 protein was absent or nonfunctional in six out of seven osteosarcoma cell lines. Both spontaneous and induced osteoblast differentiation are associated with increased $p27^{KIP1}$ mRNA and protein expression. Ectopic expression of runx2 induced an Rb- and $p27^{KIP1}$-dependent growth arrest. This was due in part to increased expression of $p27^{KIP1}$ protein, which inhibited S-phase Cdk complexes and the dephosphorylation of pRb. Interestingly, runx2 is shown to interact preferentially with the hypophosphorylated form of pRb, a known coactivator of runx2. Although $p27^{KIP1}$ expression is associated with osteoblast differentiation, loss of $p27^{KIP1}$ had only a minor effect on osteoblast differentiation in vitro and in vivo. Notably, the irreversibility of both the osteogenic phenotype and terminal cell cycle exit in vitro is dependent on expression of $p27^{KIP1}$. Immunohistochemical analysis of human osteosarcomas confirmed that expression of $p27^{KIP1}$ was lost as tumors lost evidence of osteogenic differentiation. Together, these data suggest that runx2 establishes a terminally differentiated state through Rb- and $p27^{KIP1}$-dependent mechanisms, and that these processes are disrupted in osteosarcomas.

Results

Characterization of the osteoblast phenotype in a panel of osteosarcoma cell lines

We first used transcriptional profiling to objectively characterize the differentiation state of a panel of osteosarcoma cell lines (SAOS2, MG63, B143, HOS, SJSA, and G292) relative to an osteoblast-like reference. The reference consisted of primary stromal stem cells in which expression of markers of the mature osteoblast phenotype was induced by culture in the presence of ascorbic acid, dexamethasone, and inorganic phosphate (Gronthos et al., 2003). These markers include runx2, osterix, osteocalcin, and the ability to mineralize in vitro. Consistent with a transformed state, several putative oncogenes, including FOS and cyclins A1, B2, E1, and D1 (Fig. 1 A), were commonly overexpressed in osteosarcoma cell lines, whereas the Cdk inhibitors $p16^{INK4A}$ and $p57^{KIP2}$ were relatively underexpressed. Shown in Fig. 1 A is the expression pattern of 16 bone-related genes selected from a previously published microarray study on the osteoblast phenotype (Balint et al., 2003). Twelve genes, including the key osteoblast transcription factor, *RUNX2*, were underexpressed across all osteosarcoma cell lines relative to our osteoblastic reference. Osteocalcin, a late and specific osteoblast marker not represented on our arrays, was undetectable by RT-PCR in the osteosarcoma lines (not depicted). Overall, the average median expression of 16 osteoblast-related genes in the osteosarcoma cell lines was reduced to 38 ± 8% of the osteoblastic reference.

The pattern of gene expression observed in osteosarcomas suggests a loss or reduction in activity of runx2, a key transcriptional regulator of osteoblast differentiation. To assess activity of the runx2 pathway in the osteosarcoma cell lines, we measured endogenous runx2 transcriptional activity using an osteoblast-specific promoter–luciferase construct, 6ose2-luc (Ducy and Karsenty, 1995), consisting of six tandem repeats of the osteocalcin runx2 binding site. A mutant control containing a dinucleotide substitution in the runx2 binding sites was used, abolishing runx2 binding and activity (Ducy and Karsenty, 1995). The ratio of wild-type to mutant reporter activity therefore reflects endogenous runx2 function, and it was markedly reduced in all seven osteosarcoma cell lines, to levels comparable to that observed in fibroblasts (CCL-7625; Fig. 1 B). A positive control derived from an osteogenic osteoma (CCL-7672) demonstrated runx2 activity 80-fold higher than in CCL-7625 cells. Similar results were observed with native osteopontin and osteocalcin promoter–luciferase constructs (unpublished data). The effect of ectopically expressing the osteoblast-specific MASN isoform of runx2 (hereafter runx2) on reporter activity was studied (Fig. 1 C). Ectopic expression of runx2 increased reporter activity 10–60-fold in some osteosarcoma cell lines, suggesting that endogenous levels of runx2 were limiting for transcriptional activity in these cell lines.

Lack of correlation between runx2 protein levels and transcriptional activity

There was little or no correlation between runx2 protein levels and transcriptional activity. Immunoblot analysis of endogenous runx2 protein demonstrated low levels in five out of seven cell lines (Fig. 1 D, top and middle). The upper band represents the MRIPV isoform of runx2, whereas the faster migrating band in SAOS2 represents the osteoblast-specific MASN isoform (unpublished data). The MRIPV isoform strongly induces AP activity but not osteocalcin, whereas the MASN isoform more potently activates osteocalcin but not AP (Harada et al., 1999). Consistent with the results of the transcriptional assays, no runx2 protein was detectable by Western blot in G292 cells, which showed the greatest induction of transcription by ectopic runx2 (Fig. 1 D). In contrast, abundant endogenous runx2 protein was present in SAOS2 cells. The striking contrast between protein levels and intrinsic activity of runx2 in SAOS2 cells is highlighted by comparison with protein levels in the osteoblastic control, although osteoblast gene expression is 5.6 ± 2.9–fold higher in the reference than in SAOS2 cells. We have confirmed that no mutations exist in the genomic sequences of runx2 in SAOS2 cells or any other cell line in this study. Thus, some osteosarcomas, such as G292, appear to lack functional runx2, whereas others, such as SAOS2, appear unable to activate transcription of runx2-dependent genes even when ectopic runx2 is supplied. Interestingly, we observed that all lines responsive to ectopic runx2 express pRb, whereas those that fail to respond express no or low levels of this known runx2 coactivator. Furthermore, some pRb-positive cell lines show only limited activation in response to runx2 expression, suggesting

Published December 6, 2004

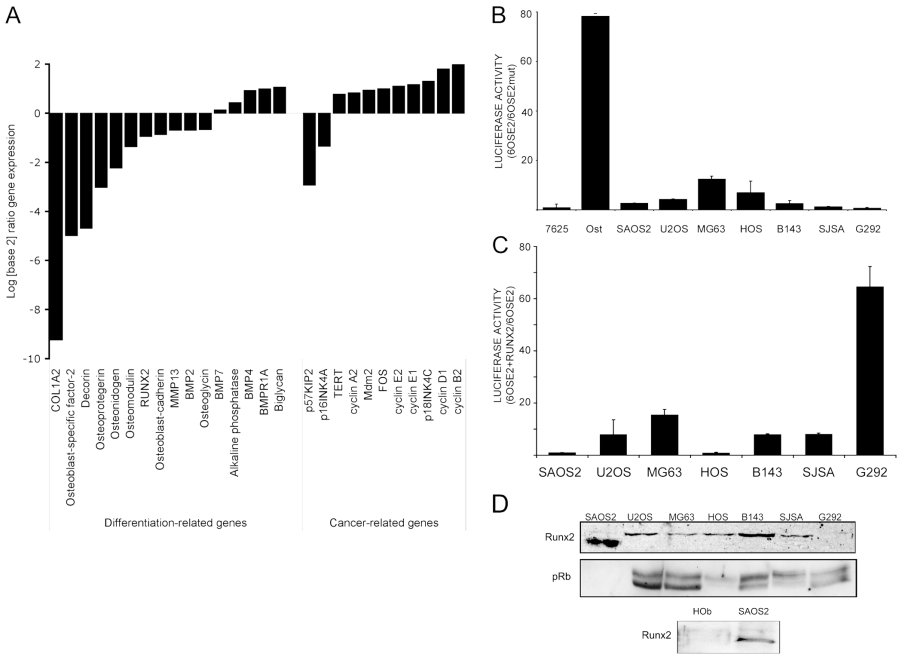

Figure 1. **Runx2-dependent osteogenic differentiation is disrupted in osteosarcoma cell lines.** (A) Gene expression arrays were performed using RNA extracted from confluent cultures of SAOS2, MG63, HOS, B143, SJSA, and G292 cell lines, normalized to reference RNA as described in Materials and methods section. Data presented are the median log-transformed data for six cell lines. (B) Cells were transfected with 6ose2-luc (or with 6ose2mut-luc) and cytomegalo virus (CMV)–βgal plasmids. After 24 h, luciferase activity was measured and normalized to β-galactosidase. The ratio of the activity of 6ose2-luc to 6ose2mut-luc activity is shown. Ost, osteogenic osteoma cell line CCL-7672. Data shown are means ± SEM. (C) Cells were transfected with 6ose2-luc and CMV-βgal plasmids, with or without a runx2 expression vector. After 24 h, luciferase activity was measured and normalized for transfection efficiency with β-galactosidase. The ratio of luciferase activity in the presence or absence of runx2 is shown. Data shown are means ± SEM. (D) Western blot for runx2 and pRb in nuclear extracts from the indicated cell lines. HOb, human primary osteoblast.

that additional factors influence the activity of runx2 in osteosarcoma cell lines (Fig. 1 D). Together, these data confirm gathering evidence that runx2 activity is critically dependent on cofactors or posttranslational modifications, and that oncogenic transformation results in consistent dysregulation of runx2 activity by multiple mechanisms.

Runx2 inhibits cell growth through p27^{KIP1} and pRb

It appears that normal runx2 function is incompatible with malignant transformation of osteoblastic cells. To determine why, we examined the effect of reexpression of runx2 in G292 cells. As shown in Fig. 1 (B and C), in G292 cells runx2 levels appeared to be rate limiting for transcriptional activity. This suggests that the molecular apparatus for full runx2 activity, including any potential tumor suppressor functions, exists in G292 cells. Consistent with this idea, ectopic expression of runx2 suppressed cell growth (Fig. 2 A). In contrast, this effect was not seen in SAOS2 cells, in which forced expression of runx2 had little effect on transcriptional activity. Because SAOS2 lacks functional pRb, whereas G292 has wild-type pRb, we hypothesized that the lack of pRb may account for the inability of runx2 to reduce the proliferative capacity of these cells. Indeed, when overexpressed in wild-type and $RB^{-/-}$ 3T3 cell lines, runx2 suppressed colony numbers of 3T3 cells by 60–90%, an effect dependent on pRb (unpublished data). To study this effect further, we used two runx2 constructs containing transactivation domain mutations. One of these (27ala) lacks transcriptional activity, whereas the other (3ala) possesses wild-type activity (Thirunavukkarasu et al., 1998). Introduction of these constructs into 3T3 cells showed that the colony suppression activity of runx2 is due to a G1 cell cycle arrest dependent on transcriptional activity and pRb (Fig. 2 B). Runx2 was ectopically expressed in primary human fibroblasts (CCL-211 and IMR90) and osteosarcoma cell lines (U2OS and SAOS2), using adenoviral vectors. As expected, runx2 inhibited the S-phase fraction of fibroblastic but not osteosarcoma cells. Initial studies of cell cycle protein expression in these transfected cells revealed a specific induction of p27^{KIP1} protein but no effect on p21^{CIP1} (Fig. 2 C). Coimmunoprecipitation from CCL-211 cells showed that p27^{KIP1} was strongly associated with cyclin A and Cdk2 (Fig. 2 D), suppressed in vitro kinase activity of cyclin A–Cdk2 complexes (Fig. 2 E), and was accompanied by dephosphorylation of endogenous pRb (Fig. 2 E). We have shown previously that pRb binds and coactivates runx2 (Thomas et al., 2001). We hypothesized that a feed-forward loop, integrating progressive cell cycle withdrawal and differentiation, would be completed if runx2 specifically interacted with the hypophosphorylated form of pRb. This is the case (Fig. 2 F). Collectively, these data are consistent with the transcriptional induction of growth arrest by runx2 through an Rb- and p27^{KIP1}-dependent mechanism that is reinforced by coactivation of runx2 by direct interactions with the hypophosphorylated form of pRb.

A role for p27^{KIP1} in osteogenic differentiation

The data described above suggest a role for p27^{KIP1} and pRb in mediating runx2-dependent proliferation arrest. We have previously reported a role for pRb in runx2-dependent expression of differentiation-related genes, and so wished to determine the physiologic significance of p27^{KIP1} in osteoblast differentiation. As reported previously (Drissi et al., 1999), osteoblast differentiation in vitro is associated with increased expression of p27^{KIP1} (Fig. 3 A). Bone morphogenetic proteins (BMPs) are powerful osteoinductive agents whose effects are mediated by runx2 (Tsuji et al., 1998; Gori et al., 1999). Treatment of murine embryonic fibroblasts (MEFs) with a synthetic BMP4/7 fusion protein induced osteoblast differentiation (and cell cycle

Published December 6, 2004

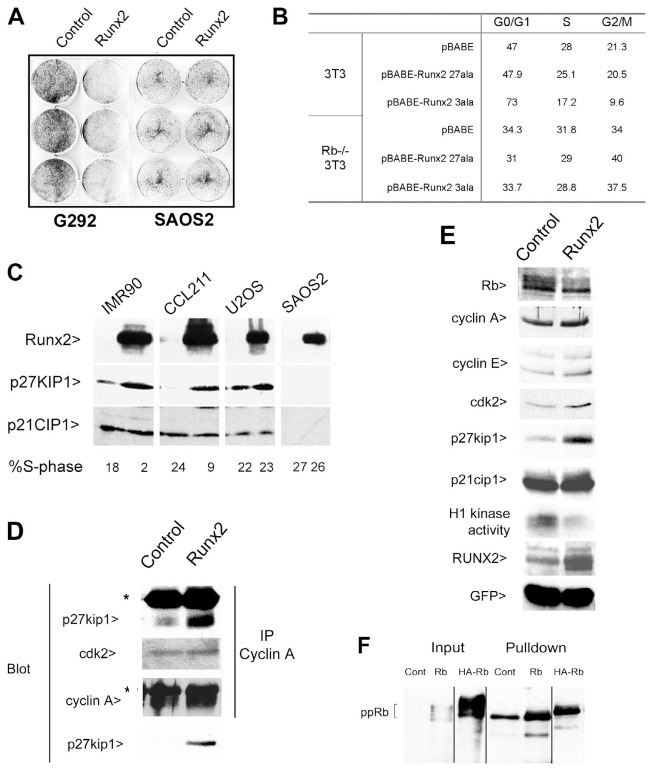

Figure 2. **Runx2 induces a growth arrest through induction of p27^{KIP1}.** (A) Effect of ectopic expression of runx2 on colony suppression assay. (B) Retroviral vectors expressing runx2 27ala or runx2 3ala were used to infect 3T3 or *RB*$^{-/-}$ 3T3 cells, followed by selection for 3 d in 2 μg/ml puromycin. Cell cycle profile was determined by flow cytometry. (C) IMR90, CCL-211, SAOS2, and U2OS cells were infected with adenoviral constructs expressing FLAG-tagged runx2. Western blot for runx2, p27^{KIP1}, and p21^{CIP1}. The percentage of cells in S-phase, derived from parallel cultures subjected to DNA analysis by flow cytometry, is indicated (bottom). (D) CCL-211 cells were infected with adenoviral constructs expressing runx2. Cyclin A immunoprecipitates were subjected to Western blot for p27^{KIP1}, Cdk2, and cyclin A. The bottom panel is directly blotted for p27^{KIP1}. Asterisks indicate Ig heavy chain bands. (E) Cyclin A immunoprecipitates assayed for kinase activity in the presence of runx2. CCL-211 cells were treated as in C. Direct Western blot for Rb, cyclin A, cyclin E, Cdk2, p27^{KIP1}, p21^{CIP1}, runx2, and GFP to demonstrate equal titers of virus in each culture. (F) Runx2 binds the hypophosphorylated form of pRb. COS-7 cells were transfected with vector, pRb, and HA-tagged pRb. A pulldown was performed using GST-runx2. Input is 5% of that used for the pulldown. ppRb, phosphorylated species of pRb. Black lines indicate that intervening lanes have been spliced out.

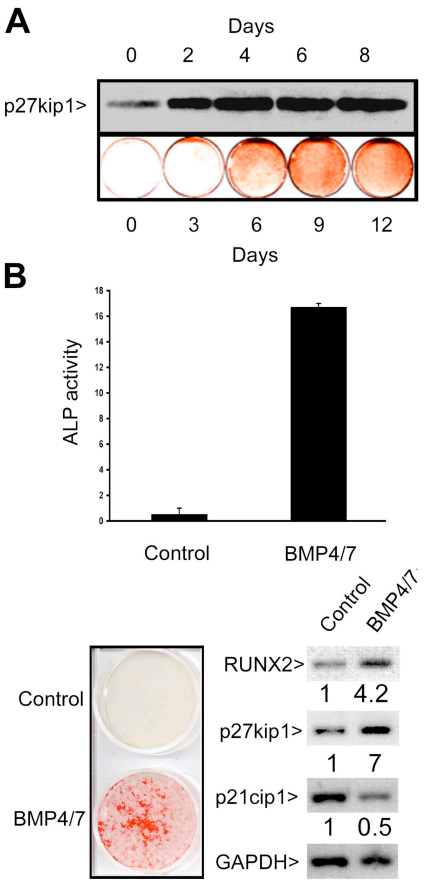

Figure 3. **Osteogenic differentiation in vitro is associated with induction of p27^{KIP1} mRNA and protein.** (A) MC3T3E1 cells were cultured in differentiation media containing 50 μg/ml ascorbic acid and 2 mM β-glycerophosphate. (top) Western blot of p27^{KIP1} protein after 2–8 d in differentiation media. (bottom) Alizarin red staining of mineralized cultures over 3–12 d under identical conditions. (B) Murine embryonic fibroblasts (MEFs) cultured in the presence of a BMP4/7 fusion protein for 14 d. (top) Induction of AP activity. Data shown are means ± SEM. (bottom left) Alizarin red staining for mineralization. (bottom right) RT-PCR for runx2, p27^{KIP1}, p21^{CIP1}, and glyceraldehyde phosphate dehydrogenase (GAPDH). Fold changes in gene expression relative to GAPDH are given below each panel.

arrest), concomitant with expression of runx2 and p27^{KIP1} mRNA (Fig. 3 B). Similarly, BMP2 induced a G1 cell cycle arrest in MEFs that was dependent in part on the presence of both pRb and p27^{KIP1} (Fig. 4 A). This is consistent with a role for runx2 in inhibition of cell proliferation and induction of differentiation by BMPs. To confirm these observations in a preosteoblast cell model, we used siRNA to knockdown p27^{KIP1} in MC3T3E1 cells (Fig. 4 B). The level of knockdown achieved was >75%, which we consider significant because p27^{KIP1} is believed to act as a haploinsufficient tumor suppressor gene (Fero et al., 1998). Consistent with observations that runx2-null osteoblasts have increased rates of proliferation (Pratap et al., 2003), we observed an increased rate of proliferation in MC3T3E1 cells in which p27^{KIP1} was reduced. BMP2 treatment of MC3T3E1 cells expressing a control siRNA vector resulted in a 42% reduction in S-phase cells, compared with a 17% reduction in cells expressing the p27^{KIP1} siRNA (Fig. 4 C). Furthermore, as observed in G292 cells and 3T3 fibroblasts, ectopic expression of runx2 suppressed growth of MC3T3E1 cells, and this effect was abolished in cells expressing siRNA for p27^{KIP1} (Fig. 4 D; Chi square $P < 0.001$). These data suggest that p27^{KIP1}, like pRb, plays a role in regulating basal rates of proliferation in preosteoblasts and contributes to the growth arrest associated with osteoblastic differentiation.

Next, we wished to determine whether p27^{KIP1} is required for the osteoblast phenotype. Loss of p27^{KIP1} partially attenuated BMP2-induced AP activity (Fig. 5 A), and both basal and BMP2-induced expression of osteocalcin, osteopontin, and type I collagen mRNA were reduced (but not abolished by) the absence of p27^{KIP1} (Fig. 5 B). To determine the net effect of loss of p27^{KIP1} in vivo, the long bones of murine wild-type and *p27*$^{KIP1-/-}$ littermates were analyzed by histomorphometry. There was a minor effect of loss of p27^{KIP1} on the formation of

Published December 6, 2004

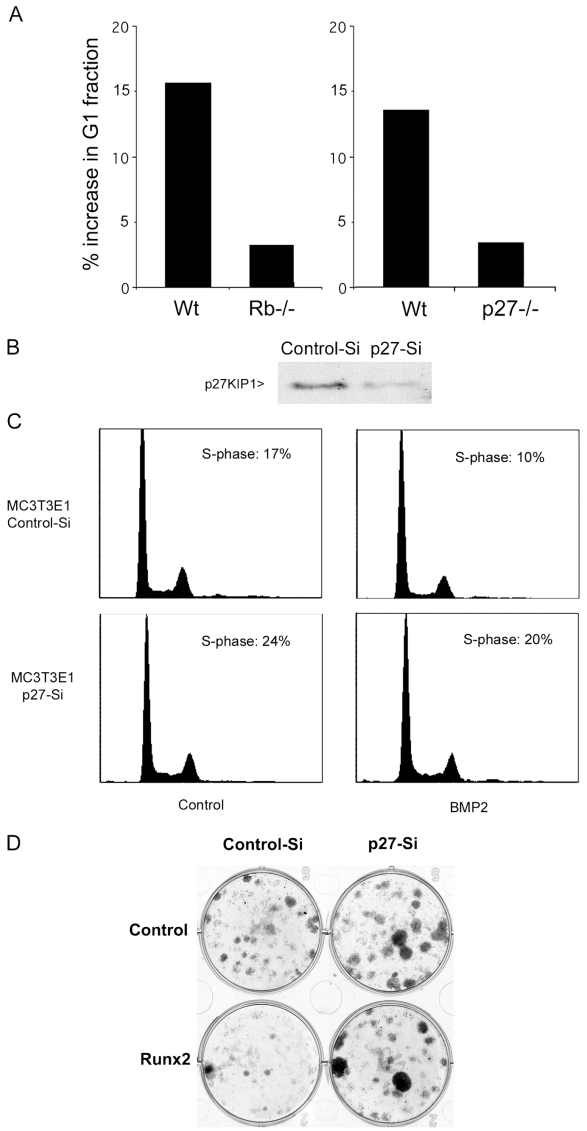

Figure 4. **Growth arrest due to expression of runx2 or treatment with BMP2 is reduced by knockdown of p27^{KIP1}.** (A) Primary MEFs of the indicated genotypes were treated with 100 ng/ml BMP2 for 48 h followed by flow cytometric analysis of DNA content. Data shown are the change in G1 fraction due to treatment. This experiment was repeated twice with similar results. (B) Western blot for p27^{KIP1} in MC3T3E1 cells infected with a retrovirus expressing either control siRNA or siRNA for p27^{KIP1}. (C) DNA analysis using flow cytometry of cultures of cells derived as described in B. (D) Colony suppression assay of cells as described transfected with empty vector or runx2. Each experiment was performed in triplicate.

unmineralized bone (osteoid), both as a function of total bone volume and as measured by osteoid thickness (Fig. 5 C). This effect was not a result of accelerated mineralization caused by loss of p27^{KIP1}, because there was no evidence of altered mineral apposition rate as measured directly by dual calcein labeling. Osteoblast and osteoclast numbers were unchanged (unpublished data). Because osteoclasts do not resorb unmineralized osteoid (Chambers et al., 1985), any defect in osteoclast function is unlikely to account for the reduction in osteoid. These data are consistent with a very minor effect of loss of p27^{KIP1} on osteoblast differentiation and function.

p27^{KIP1} is needed for terminal cell cycle egress

p27^{KIP1} plays a key role in terminal cell cycle exit in osteosarcoma cells (Alexander and Hinds, 2001). Because terminal differentiation is associated with permanent cell cycle withdrawal, we tested whether MEF cultures lacking p27^{KIP1} could reenter the cell cycle after culture under prolonged differentiating conditions. There was no prior difference in cell cycle profile of littermate wild-type or *p27$^{KIP1-/-}$* preconfluent early passage MEFs (unpublished data). However, although wild-type MEFs postdifferentiation grew poorly after passage, MEFs lacking p27^{KIP1} proliferated robustly (Fig. 6 A). This suggests a role for p27^{KIP1} in mediating the irreversibility of the postconfluent state. However, wild-type undifferentiated MEFs also failed to reenter the cell cycle, probably because p27^{KIP1} also accumulated in untreated cultures upon confluence (Hirano et al., 2001; and unpublished data). Consistent with an additional effect of BMP2 upon p27^{KIP1}, the degree of growth inhibition after passage was greater in cultures treated with BMP2 (Fig. 6 A). Moreover, even postdifferentiated MEFs lacking p27^{KIP1} demonstrated a reduction in cell growth when passaged after BMP2 treatment, indicating that p27^{KIP1} contributes to (but is not solely responsible for) terminal growth arrest. We have not observed compensatory increases in p21^{CIP1} or p57^{KIP2} in p27^{KIP1}-null cultures (unpublished data), and the mechanisms accounting for the residual effects are not known.

Reentry into the cell cycle of BMP2-treated cultures was associated with loss of differentiation. Compared with wild-type cultures, BMP2-treated p27^{KIP1}-null cultures rapidly lost expression of osteocalcin within 2 d of passage (Fig. 6 B). Additionally, the number of AP-positive cells was >20-fold greater in wild-type compared with *p27$^{KIP1-/-}$* cultures (4.8 ± 1.8% [n = 263, 10 high-power fields], compared with 0.2 ± 0.1% AP-positive cells [n = 2039]). This suggests that terminal cell cycle exit, in this case dependent on p27^{KIP1}, is required for maintenance of the differentiated state.

Permanent cell cycle withdrawal is a feature of both senescence and terminal differentiation (Goldstein, 1990; Sellers et al., 1998). Postdifferentiated wild-type MEFs assumed a binucleated, enlarged, flattened morphology reminiscent of replicative senescence. Whether differentiated or not, significant numbers of postconfluent wild-type MEFs stained for senescence-associated β-galactosidase activity (Dimri et al., 1995). This effect was greater in cultures that had been treated with BMP2 (Fig. 6 D). In contrast, MEFs lacking p27^{KIP1} did not stain for senescence-associated β-galactosidase and morphologically resembled undifferentiated cultures. Although the effects of both BMP2 and p27^{KIP1} were independently statistically significant, the interaction between these factors failed to reach significance, perhaps because of the powerful effect of confluence on accumulation of p27^{KIP1} in both treated and control cultures. Together, these data suggest that culture conditions required for differentiation of MEFs (including both BMP2 treatment and prolonged confluence), as well as expression of p27^{KIP1}, contribute to the entry of MEFs into a senescence-like state.

Published December 6, 2004

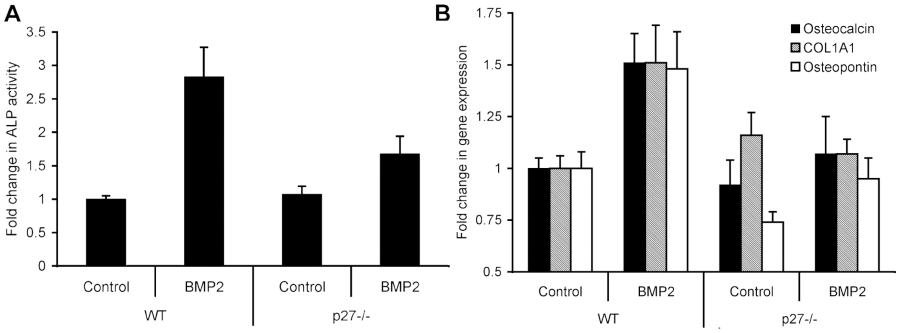

C

	Bone volume/ Total volume (%)	Osteoid volume/ Bone volume (%)	Osteoid thickness (μm)	Mineral apposition rate (μm/day)	Osteoblasts/ bone perimeter (#/mm)
p27+/+	5.8±0.5 (n=12)	4.06±0.95 (n=10)	2.36±0.19 (n=10)	1.58±0.07 (n=5)	18.7±2.4 (n=10)
p27-/-	7.6±0.7 (n=13)	**1.96±0.32** (n=9)	**1.84±0.18** (n=9)	1.5±0.06 (n=8)	18.1±1.6 (n=9)

Figure 5. **Role of p27^{KIP1} in osteoblast function.** (A) MEFs of the indicated genotypes were differentiated in the presence of 100 ng/ml BMP2, ascorbic acid, and β-glycerophosphate for 7 d and analyzed for AP activity. Data shown are means ± SEM of fold change relative to untreated wild-type controls ($n = 4$ experiments using independently derived littermate-matched cultures, each in triplicate). Genotype effect significant by analysis of variance (ANOVA; $P < 0.01$). (B) RT-qPCR analysis of gene expression in MEFs of the indicated genotypes, normalized to ARPP$_o$. Data shown are means ± SEM. Genotype effect significant for BMP2 induction of osteocalcin ($P < 0.01$) and type I collagen ($P < 0.05$, ANOVA), but not osteopontin. (C) Histomorphometric analysis of long bones in mice between 8 and 12 wk old of the indicated genotypes. Data shown are means ± SEM. Bold-faced data are significantly different from wild-type littermates ($P < 0.05$).

Expression of p27^{KIP1} is lost in osteosarcoma

We finally wished to determine whether these observations have relevance to human osteosarcoma. p27^{KIP1} expression appears to be key for cell cycle withdrawal and terminal differentiation in osteoblasts, and integrates the functions of BMPs, pRb, and runx2 in these processes. Regardless of the nature of the defect in the pRb–runx2 pathway in osteosarcoma cells, the net effect will be loss of growth restraint due to diminished expression of p27^{KIP1}. Consistent with this, we found negligible expression of p27^{KIP1} protein in high-grade osteosarcoma cells, although p27^{KIP1} was clearly seen in osteoclasts as reported previously (Okahashi et al., 2001; Fig. 7, A and D), correlating inversely with expression of proliferating cell nuclear antigen (PCNA; Fig. 7, D and F, arrows). These high-grade osteosarcomas demonstrated frequent mitotic figures and little differentiation, as evidenced by osteoid production and osteocalcin expression (Fig. 7, B and E). High-grade tumor cells expressed high levels of PCNA, consistent with a high S-phase fraction (Fig. 7, C and F). In contrast, in lower grade tumors with mineralizing osteoid and lower cellularity with more normal osteoblastic morphology, expression of both p27^{KIP1} and osteocalcin is evident, especially in terminally differentiated (PCNA negative) osteocytes embedded within bone (Fig. 7, G and H, arrows). Critically, there was a significant relationship between expression of p27^{KIP1} protein and osteoblast differentiation scored by osteoid production in a panel of 100 osteosarcomas (Fig. 7 J, $P < 0.05$). This effect was independent of proliferative rate, because there was no significant relationship between PCNA expression and p27^{KIP1}. These data support the view that the loss of differentiation of osteosarcomas, which conveys adverse prognostic significance, is associated with loss of expression of p27^{KIP1}.

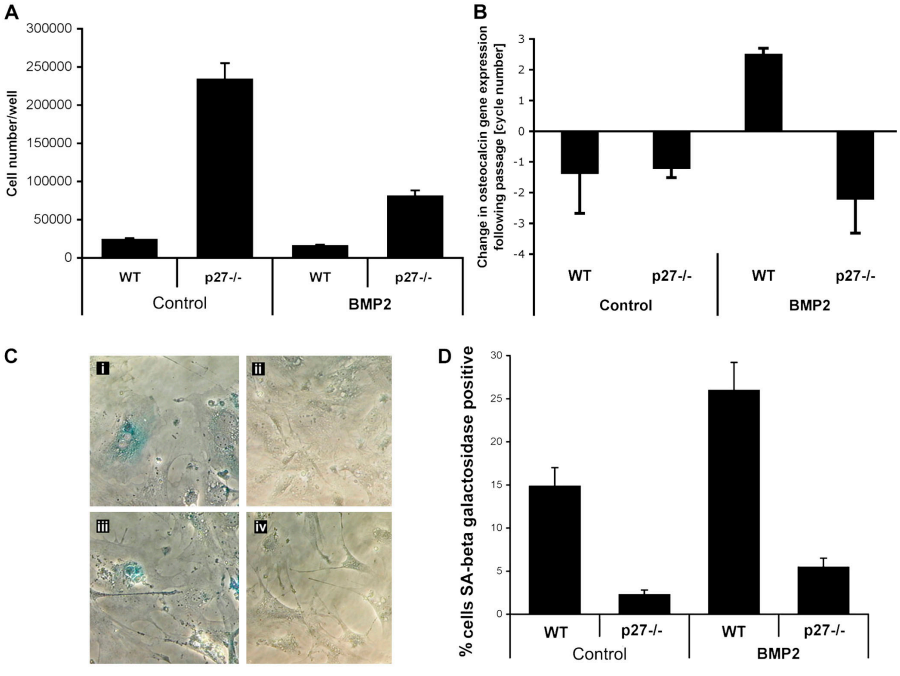

Figure 6. **p27^{KIP1} is required for terminal growth arrest in vitro.** MEFs were cultured in the presence or absence of 100 ng/ml BMP2, ascorbic acid, and β-glycerophosphate for 14 d after confluence. Cells were then passaged. (A) 5×10^4 cells were grown under standard culture conditions for 3 d, and then counted. Data shown are means ± SEM. (B) RT-qPCR analysis of osteocalcin gene expression in MEFs of the indicated genotypes 2 d after passage. Data shown are means ± SEM of cycle number (ΔΔCT) normalized to ARPP$_o$ and expression before passage. The interaction between BMP2 and genotype was significant ($P < 0.01$, ANOVA). (C) Photomicrograph of senescence-associated β-galactosidase–stained cultures. (i) Wild-type untreated cultures; (ii) *p27$^{KIP1-/-}$* untreated cultures; (iii) wild-type differentiated cultures; and (iv) *p27$^{KIP1-/-}$* differentiated cultures. (D) Cells were stained for senescence-associated (SA) β-galactosidase activity after passage and counted (>200 cells in triplicate cultures). Data shown are means ± SEM. The effect of BMP2 and genotype was significant ($P < 0.01$), although there was no interaction by ANOVA.

Published December 6, 2004

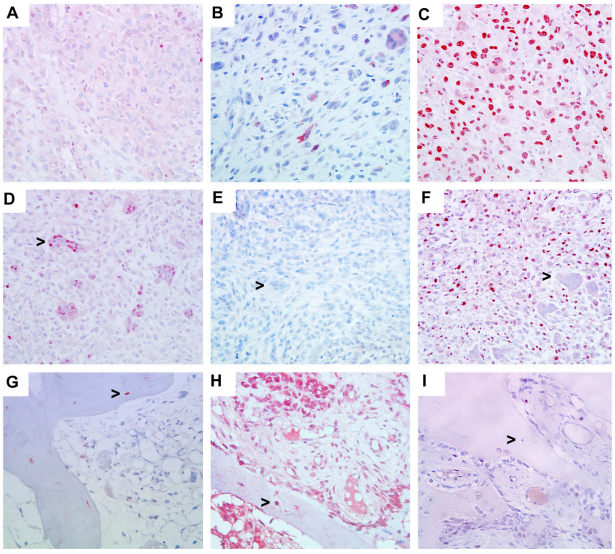

Figure 7. **Expression of p27^{KIP1}, osteocalcin, and proliferating cell nuclear antigen (PCNA) in human osteosarcoma samples.** (A–I) High-power photomicrographs of parallel sections from two high-grade (A–C and G–I) and one low-grade (G–I) human osteosarcomas were stained for p27^{KIP1} (A, D, and G), osteocalcin (B, E, and H), and PCNA (C, F, and I). Arrows in D–F indicate multinucleated osteoclast; arrows in G–I indicate osteocytes. Bar, 50 μm. (J) Blinded quantitation of staining for p27^{KIP1} and PCNA in tumors with evidence of osteoblast differentiation (osteoid production) compared with dedifferentiated tumors. Error bars represent SEM. *, $P < 0.05$.

Discussion

The inverse relationship between proliferation and differentiation in osteoblasts has been carefully documented for many years, although the mechanisms have not been delineated. These observations have led to the proposition that full expression of the osteoblast phenotype is necessarily associated with terminal cell cycle exit (Stein et al., 1996; Aubin, 1998). In accord with these observations, osteoblasts lacking functional runx2 appear to lose a growth restraint (Pratap et al., 2003). Our data provide a mechanistic basis for these observations (Fig. 8). Osteogenic differentiation in culture imposes a growth restraint and, eventually, a terminal cell cycle exit resembling senescence, through runx2-dependent induction of p27^{KIP1}. We and others show that osteogenic differentiation in vitro is associated with increased expression of p27^{KIP1} (Drissi et al., 1999). This leads to a pRb-dependent growth arrest through inhibition of S-phase cyclin complexes. We have shown previously that interactions between runx2 and pRb enhance runx2-dependent transcriptional activity (Thomas et al., 2001). Because it is the hypophosphorylated form of pRb that binds runx2, the induction of p27^{KIP1} will enhance the transactivation of runx2 by pRb, leading to progressive growth arrest and expression of the mature osteoblast phenotype (Fig. 8). It is likely that loss of function of any component of this feed-forward loop will disrupt both differentiation and a restraint on cell growth. Although mutations have been documented in pRb in osteosarcoma, the molecular events that affect runx2 function in cell lines in which pRb is not affected remain unknown.

We observed a very minor defect in osteoid synthesis in *p27$^{KIP1\,-/-}$* mice, accompanied by defects in BMP2-induced differentiation in vitro, consistent with apparently normal skeletal patterning in mice nullizygous for p27^{KIP1} (Fero et al., 1996; Kiyokawa et al., 1996; Nakayama et al., 1996). It is possible that functional redundancy allows compensation for loss of p27^{KIP1}, and consistent with this hypothesis, BMP2 induced an attenuated growth arrest in p27^{KIP1}-null fibroblasts. Although the mechanisms by which BMP2 induces a growth arrest in the absence of p27^{KIP1} are not known, BMP2 and runx2 have both overlapping and distinct effects to promote osteoblast differentiation. In addition to inducing p27^{KIP1}, BMP2 has recently been reported to inhibit Cdk6 levels by a SMAD-dependent mechanism (Ogasawara et al., 2004).

The induction of p27^{KIP1} leads to more than a simple proliferative arrest. Although the proliferation of early passage MEFs was not strikingly affected by loss of p27^{KIP1} (Fero et al., 1996; Kiyokawa et al., 1996; Nakayama et al., 1996; and unpublished data), we found that p27^{KIP1} was required to maintain a growth-arrested state in differentiated cells. p27^{KIP1} has been suggested previously to be a part of the normal timer that determines the cessation of proliferation and commitment to differentiation of oligodendrocyte precursors (Casaccia-Bonnefil et al., 1997; Durand et al., 1998). The *Drosophila melanogaster* p27^{KIP1} homologue, *dacapo*, initiates terminal cessation of cell division and differentiation, an effect that interacts genetically with pRb (de Nooij et al., 1996; Lane et al., 1996). These data suggest that p27^{KIP1} may act as a "fate switch" that, once expressed at sufficient levels, commits the osteoblast to a postmitotic state. Irreversible cell cycle exit is a feature of senescence, in which p27^{KIP1} plays a role and which may represent a defense to oncogenic transformation (Serrano et al., 1997; Sellers

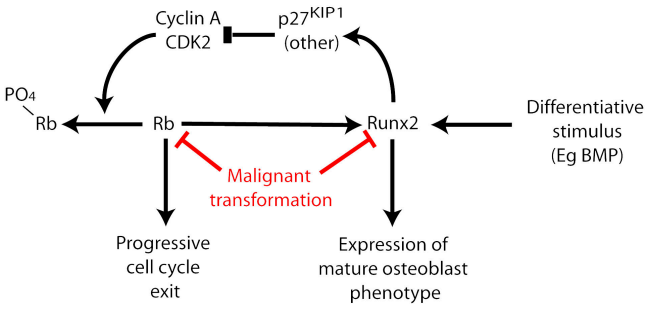

Figure 8. **A model for interactions between cell cycle proteins and runx2 in osteoblasts.** The interaction of hypophosphorylated pRB with runx2 completes a positive feedback loop, promoting cell cycle withdrawal and expression of the osteoblast phenotype. See Discussion section.

Published December 6, 2004

et al., 1998; Alexander and Hinds, 2001; Thomas et al., 2001). Clearly, terminal cell cycle exit, whether in response to differentiation or to oncogenic events, is fundamentally inconsistent with oncogenic transformation.

Does $p27^{KIP1}$ act as a tumor suppressor in bone? In animal models, loss of $p27^{KIP1}$ is associated with infrequent spontaneous pituitary tumors and intestinal adenomas but accelerates the rate of tumor formation when combined with carcinogen exposure (Fero et al., 1998) or mutations to *TP53* (Philipp-Staheli et al., 2004). Interestingly, osteosarcomas were observed in this latter study, albeit at low frequency. Consistent with a role for $p27^{KIP1}$ in osteosarcoma, the protooncogene c-Fos, which causes osteosarcoma in mice (Grigoriadis et al., 1993), induces cyclin A–Cdk2 activity and represses $p27^{KIP1}$ in osteoblasts (Sunters et al., 2004). Unusually, $p27^{KIP1}$ appears to act as a haploinsufficient tumor suppressor in the mouse (Fero et al., 1998), and, where human tumors have undergone a loss-of-heterozygosity event, silencing of the remaining allele is rare (Kawamata et al., 1995; Ponce-Castaneda et al., 1995). This may be due to the dual role of $p27^{KIP1}$ as an assembly factor for G1-phase cyclin complexes as well as a stoichiometric inhibitor of S-phase cyclin complexes (Sherr and Roberts, 1999). Importantly, decreases in $p27^{KIP1}$ protein expression have been found in 60% of human carcinomas (Slingerland and Pagano, 2000), and are associated in breast cancer with poor prognosis (Fredersdorf et al., 1997). Our clinical studies reveal an association between $p27^{KIP1}$ expression and loss of differentiation in human osteosarcomas, independent of rates of proliferation per se (Fig. 7). Loss of differentiation in sarcomas in general is a marker of high-grade status, which in turn is associated with worse prognosis.

Disruption of runx2-dependent transcriptional activity is common in osteosarcoma cell lines and leads in a clinically measurable fashion to loss of both differentiation and expression of $p27^{KIP1}$ in human osteosarcomas. Although the specific mechanisms contributing to the loss of function of runx2 are not understood, global demethylation of osteosarcoma cell lines results in reactivation of differentiation concomitant with reversion of transformation (unpublished data). Methylation is a well-described, common method of silencing tumor suppressor pathways (Baylin and Herman, 2000), and the restoration of differentiation by demethylation further supports the notion that tumors gain a selective survival advantage by silencing differentiation-related growth inhibitory processes. We hope that identifying targets of methylation-induced silencing will shed additional light on the interactions between differentiation and cell cycle exit.

Materials and methods

Cell lines and reagents

The osteosarcoma cell lines were maintained in DME (GIBCO BRL) containing 15% FCS. CCL-7625 and CCL-7672 cells were obtained from American Type Culture Collection. MC3T3E1 cells were maintained in MEM supplemented with 10% FCS. $RB^{-/-}$ 3T3 and NIH3T3 cells were infected with pBABEpuro retrovirus (Morgenstern and Land, 1990) expressing mutant constructs of runx2 (Thirunavukkarasu et al., 1998), and with pooled clones selected with puromycin. Stable expression of constructs was confirmed by immunoblot (unpublished data). Wild-type and $RB^{-/-}$ MEFs with the described genotypes (wild-type and $RB^{-/-}$) were derived from matched littermates (gifts of T. Jacks, Massachusetts Institute of Technology, Boston, MA), and $p27^{KIP1-/-}$ mice were obtained from J. Roberts (Fred Hutchinson Cancer Research Center, Seattle, WA) (Fero et al., 1996). Mineralization was induced by culture in the presence of 5 mM β-glycerophosphate and 50 μg/ml ascorbic acid for 3 wk after confluence (Thomas et al., 2001). For colony suppression assays, cells (10^5/10-cm plate) were transfected with constructs as indicated in Figs. 2 A and 4 D. After 24 h, cells were selected in the presence of antibiotic (2 μg/ml puromycin or 1–5 μg/ml neomycin) for 14–21 d. Colonies were visualized with crystal violet. Doses of 5-aza-2-deoxycytidine were titrated in preliminary studies for each cell line to achieve growth arrest without significant cell death, usually between 2 and 5 μM.

SV-Rb and SV-HARb were used for the expression of full-length pRb (Hinds et al., 1992). Expression constructs for runx2 were cloned into pBABEpuro (Morgenstern and Land, 1990). The retrovirus was amplified and purified in amphotropic packaging cell line Phoenix 293 (courtesy of G. Nolan, Stanford University, Palo Alto, CA), according to the method of Pear et al. (1993). Plasmids were transfected into cells with the use of Fugene, according to the manufacturer's instructions (Roche Pharmaceuticals). Adenoviral constructs expressing pRb and runx2-FLAG were generated as reported previously (Thomas et al., 2001).

Cell-based assays

Luciferase assays were performed according to manufacturer's instructions (Promega). Where indicated (Fig. 1, B and C), results were normalized for transfection efficiency with β-galactosidase activity or protein content. AP activity was assayed as described previously (Sellers et al., 1998). Assays for mineralization were performed as described previously (Thomas et al., 2001). Quantitation was performed by dissolving stained mineralized cultures in 10% cetylpyridinium chloride, followed by spectrophotometric analysis at 540 nm. Both AP activity and mineralization were normalized to protein content (Bio-Rad Laboratories). Flow cytometry for DNA content was performed as described previously (Thomas et al., 2001).

RT-PCR analysis of gene expression

RNA was extracted with the use of TRIzol (Invitrogen), according to the manufacturer's instructions. cDNA was produced from 1 μg of total RNA with the use of a commercially available kit (SUPERSCRIPT Choice system for cDNA synthesis; GIBCO BRL). Semiquantitative PCR analysis was performed after optimization. Primer sequences and PCR conditions are available on request. For quantitative RT-PCR, expression of each target gene was normalized to expression of $ARPP_0$ with the use of an ABI-Prism 7700 Light Cycler and SYBR Green. Optimal PCR conditions were established for each gene in preliminary experiments.

Analysis of protein expression and kinase assays

Nuclear extracts and immunoblot analyses were performed as described previously (Thomas et al., 2001). The following antibodies were used: anti-FLAG antibody (M2; Sigma-Aldrich); human pRb: monoclonal antibody 245 (BD Biosciences); runx2: M-70 (Santa Cruz Biotechnology, Inc.); $p27^{KIP1}$: K25020 (Transduction Laboratories); and cyclin E: HE12, cyclin A: H432, and Cdk2: M2 (Santa Cruz Biotechnology, Inc.). Horseradish peroxidase–conjugated secondary antibodies were used (Jackson ImmunoResearch Laboratories) and signal was detected by ECL (NEN Life Science Products). The GST-runx2 pulldown studies shown in Fig. 4 D were performed as described previously (Thomas et al., 2001). Kinase assays were performed as described previously (Alexander and Hinds, 2001). Cyclin A was immunoprecipitated using agarose-conjugated antibody BF683 (Upstate Biotechnology).

Immunohistochemistry

25 paraffin-embedded osteosarcoma samples were obtained from the pathology archives at St. Vincent's Hospital Melbourne, with approval from the Human Research Ethics Committee. 2-mm cores were punched and then assembled into a tissue microarray. Sections were cut at 3 μm and mounted onto Superfrost Plus slides. Primary antibodies were incubated for 30 min. For $p27^{KIP1}$, clone SX53G8 (DakoCytomation) was used at 1:50. A predilute monoclonal antibody to human osteocalcin (OC-1; Biogenex) was used at 1:4. For PCNA, clone PC10 (DakoCytomation) was used at 1:400. The primary antibody was detected with the mouse Envision+ system (DakoCytomation). Immunoreactivity was visualized with AEC+ chromogen (DakoCytomation), using hematoxylin as a counterstain. Samples for $p27^{KIP1}$ and osteocalcin were incubated in 10 mM boiling sodium citrate buffer, pH 6.0, for 2 min before staining.

Published December 6, 2004

Slides were imaged using a microscope (Axioskop 2; Carl Zeiss MicroImaging, Inc.) with a Plan-Neofluar objective (40×, 0.75 NA), and a cooled color digital camera (RT Slider SPOT; Diagnostic Instruments) and software (SPOT V4.0.2 for Windows). Subsequent processing of TIFF files was undertaken in Adobe Photoshop (V7.0.1). Images were cropped, labeled as indicated in Fig. 7, and assembled into composites for figures after minor adjustments for contrast and color balance were applied to all parts of each image.

Microarray analysis

Total RNA from osteosarcoma and common reference cell lines was isolated using phenol-chloroform extraction (TRIzol; Invitrogen) and purified by column chromatography (RNeasy; QIAGEN). The common reference RNA, containing pooled RNA from 11 human tumor cell lines, was prepared as described previously (Pollack, 2002). Total RNA (40–50 μg) was reverse transcribed with Moloney Murine Leukemia Virus Reverse transcriptase (Promega), in the presence of amino-allyl (AA)–modified dUTP (Sigma-Aldrich). AA-dUTP cDNA was labeled by coupling to Cy3 and Cy5 (reference and sample, respectively) monoreactive dyes (Amersham Biosciences). cDNA arrays containing ~10.5 K elements representing 9,381 unique cDNA (Unigene build 172) were produced at Peter MacCallum Cancer Centre Microarray Core facility on superamine slides (Telechem), with a robotic arrayer (Virtek/Bio-Rad Laboratories). Labeled probe was hybridized to the array in 3.1 × SSC and 50% formamide at 42°C for 14–16 h in a humidified and temperature-controlled chamber ($HyPro_{20}$; Thermo Hybaid). Slides were washed at room temperature with 0.5 × SSC/0.01% SDS (for 1 min), then with 0.5 × SSC (for 3 min), and finally with 0.06 × SSC (for 3 min). Scanning was performed with an Agilent G2565AA Microarray Scanner and data was extracted with GenePix Pro 4.1 software (Axon Instruments, Inc.). All array experiments, including cell culture, were performed independently twice. A complete list of genes is available from the authors on request. Data from each independent experiment were averaged, and then the median obtained from all six cell lines was used in the data shown in Fig. 1. Data were analyzed with GeneSpring software (Silicon Genetics), and samples were normalized with LOWESS (Yang et al., 2002).

Histomorphometry

Tibiae were collected from male *p27KIP1*$^{-/-}$ and wild-type littermates at 16 wk of age, fixed in cold 4% paraformaldehyde in PBS overnight, and embedded in methylmethacrylate (Sims et al., 2000). Double fluorochrome labeling to quantitate mineral appositional rates was performed as described previously (Sims et al., 2000). 5-μm sections were stained with toluidine blue or analyzed unstained for fluorochrome labels according to standard procedures in the proximal tibia using the Osteomeasure system (Osteometrics, Inc.). Tibial cortical thickness and periosteal mineral appositional rates were measured as described previously (Sims et al., 2000).

The authors would like to thank members of the Thomas lab and Phil Darcy for helpful discussions.

D.M. Thomas is the recipient of a National Health and Medical Research Council R.D. Wright fellowship (Regkey 251752) and is supported by the Cancer Council of Victoria. P.W. Hinds and G. Gutierrez are supported by National Institutes of Health grant AG20208.

Submitted: 30 September 2004
Accepted: 28 October 2004

References

Alexander, K., and P.W. Hinds. 2001. Requirement for p27(^{KIP1}) in retinoblastoma protein-mediated senescence. *Mol. Cell. Biol.* 21:3616–3631.

Aubin, J.E. 1998. Bone stem cells. *J. Cell. Biochem. Suppl.* 30-31:73–82.

Balint, E., D. Lapointe, H. Drissi, C. Van Der Meijden, D.W. Young, A.J. Van Wijnen, J.L. Stein, G.S. Stein, and J.B. Lian. 2003. Phenotype discovery by gene expression profiling: mapping of biological processes linked to BMP-2-mediated osteoblast differentiation. *J. Cell. Biochem.* 89:401–426.

Baylin, S.B., and J.G. Herman. 2000. DNA hypermethylation in tumorigenesis: epigenetics joins genetics. *Trends Genet.* 16:168–174.

Bodine, P.V., M. Trailsmith, and B.S. Komm. 1996. Development and characterization of a conditionally transformed adult human osteoblastic cell line. *J. Bone Miner. Res.* 11:806–819.

Casaccia-Bonnefil, P., R. Tikoo, H. Kiyokawa, V. Friedrich Jr., M.V. Chao, and A. Koff. 1997. Oligodendrocyte precursor differentiation is perturbed in the absence of the cyclin-dependent kinase inhibitor p27^{KIP1}. *Genes Dev.* 11:2335–2346.

Chambers, T.J., J.A. Darby, and K. Fuller. 1985. Mammalian collagenase predisposes bone surfaces to osteoclastic resorption. *Cell Tissue Res.* 241: 671–675.

Dahlin, D.C. 1957. Bone Tumors. Charles C. Thomas, Springfield, IL. 224 pp.

de Nooij, J.C., M.A. Letendre, and I.K. Hariharan. 1996. A cyclin-dependent kinase inhibitor, Dacapo, is necessary for timely exit from the cell cycle during *Drosophila* embryogenesis. *Cell.* 87:1237–1247.

Dimri, G.P., X. Lee, G. Basile, M. Acosta, G. Scott, C. Roskelley, E.E. Medrano, M. Linskens, I. Rubelj, and O. Pereira-Smith. 1995. A biomarker that identifies senescent human cells in culture and in aging skin *in vivo*. *Proc. Natl. Acad. Sci. USA.* 92:9363–9367.

Drissi, H., D. Hushka, F. Aslam, Q. Nguyen, E. Buffone, A. Koff, A.J. van Wijnen, J.B. Lian, J.L. Stein, and G.S. Stein. 1999. The cell cycle regulator p27(^{KIP1}) contributes to growth and differentiation of osteoblasts. *Cancer Res.* 59:3705–3711.

Ducy, P., and G. Karsenty. 1995. Two distinct osteoblast-specific cis-acting elements control expression of a mouse osteocalcin gene. *Mol. Cell. Biol.* 15:1858–1869.

Ducy, P., R. Zhang, V. Geoffroy, A.L. Ridall, and G. Karsenty. 1997. Osf2/Cbfa1: a transcriptional activator of osteoblast differentiation. *Cell.* 89: 747–754.

Ducy, P., M. Starbuck, M. Priemel, J. Shen, G. Pinero, V. Geoffroy, M. Amling, and G. Karsenty. 1999. A Cbfa1-dependent genetic pathway controls bone formation beyond embryonic development. *Genes Dev.* 13:1025–1036.

Durand, B., M.L. Fero, J.M. Roberts, and M.C. Raff. 1998. p27^{KIP1} alters the response of cells to mitogen and is part of a cell-intrinsic timer that arrests the cell cycle and initiates differentiation. *Curr. Biol.* 8:431–440.

Fero, M.L., M. Rivkin, M. Tasch, P. Porter, C.E. Carow, E. Firpo, K. Polyak, L.H. Tsai, V. Broudy, R.M. Perlmutter, et al. 1996. A syndrome of multiorgan hyperplasia with features of gigantism, tumorigenesis, and female sterility in p27(^{KIP1})-deficient mice. *Cell.* 85:733–744.

Fero, M.L., E. Randel, K.E. Gurley, J.M. Roberts, and C.J. Kemp. 1998. The murine gene p27Kip1 is haplo-insufficient for tumour suppression. *Nature.* 396:177–180.

Feuerbach, D., E. Loetscher, K. Buerki, T.K. Sampath, and J.H. Feyen. 1997. Establishment and characterization of conditionally immortalized stromal cell lines from a temperature-sensitive T-Ag transgenic mouse. *J. Bone. Miner. Res.* 12:179–190.

Fredersdorf, S., J. Burns, A.M. Milne, G. Packham, L. Fallis, C.E. Gillett, J.A. Royds, D. Peston, P.A. Hall, A.M. Hanby, et al. 1997. High level expression of p27(kip1) and cyclin D1 in some human breast cancer cells: inverse correlation between the expression of p27(kip1) and degree of malignancy in human breast and colorectal cancers. *Proc. Natl. Acad. Sci. USA.* 94:6380–6385.

Goldstein, S. 1990. Replicative senescence: the human fibroblast comes of age. *Science.* 249:1129–1133.

Gori, F., T. Thomas, K.C. Hicok, T.C. Spelsberg, and R.L. Riggs. 1999. Differentiation of human marrow stromal precursor cells: bone morphogenetic protein-2 increases OSF2/CBFA1, enhances osteoblast commitment, and inhibits late adipocyte maturation. *J. Bone Miner. Res.* 14:1522–1535.

Grigoriadis, A.E., K. Schellander, Z.Q. Wang, and E.F. Wagner. 1993. Osteoblasts are target cells for transformation in c-*fos* transgenic mice. *J. Cell Biol.* 122:685–701.

Gronthos, S., A.C. Zannettino, S.J. Hay, S. Shi, S.E. Graves, A. Kortesidis, and P.J. Simmons. 2003. Molecular and cellular characterisation of highly purified stromal stem cells derived from human bone marrow. *J. Cell Sci.* 116:1827–1835.

Harada, H., S. Tagashira, M. Fujiwara, S. Ogawa, T. Katsumata, A. Yamaguchi, T. Komori, and M. Nakatsuka. 1999. Cbfa1 isoforms exert functional differences in osteoblast differentiation. *J. Biol. Chem.* 274:6972–6978.

Hinds, P.W., S. Mittnacht, V. Dulic, A. Arnold, S.I. Reed, and R.A. Weinberg. 1992. Regulation of retinoblastoma protein functions by ectopic expression of human cyclins. *Cell.* 70:993–1006.

Hirano, M., K. Hirano, J. Nishimura, and H. Kanaide. 2001. Transcriptional upregulation of p27(^{KIP1}) during contact-induced growth arrest in vascular endothelial cells. *Exp. Cell Res.* 271:356–367.

Hopyan, S., N. Gokgoz, R.S. Bell, I.L. Andrulis, B.A. Alman, and J.S. Wunder. 1999. Expression of osteocalcin and its transcriptional regulators corebinding factor alpha 1 and MSX2 in osteoid-forming tumors. *J. Orthop. Res.* 17:633–638.

Kawamata, N., R. Morosetti, C.W. Miller, D. Park, K.S. Spirin, T. Nakamaki, S. Takeuchi, Y. Hatta, J. Simpson, S. Wilcyznski, et al. 1995. Molecular analysis of the cyclin-dependent kinase inhibitor gene p27/Kip1 in human malignancies. *Cancer Res.* 55:2266–2269.

Kiyokawa, H., R.D. Kineman, K.O. Manova-Todorova, V.C. Soares, E.S. Hoffman, M. Ono, D. Khanam, A.C. Hayday, L.A. Frohman, and A. Koff.

1996. Enhanced growth of mice lacking the cyclin-dependent kinase inhibitor function of p27(^{KIP1}). *Cell.* 85:721–732.

Komori, T., H. Yagi, S. Nomura, A. Yamaguchi, K. Sasaki, K. Deguchi, Y. Shimizu, R.T. Bronson, Y.H. Gao, M. Inada, et al. 1997. Targeted disruption of Cbfa1 results in a complete lack of bone formation owing to maturational arrest of osteoblasts. *Cell.* 89:755–764.

Lane, M.E., K. Sauer, K. Wallace, Y.N. Jan, C.F. Lehner, and H. Vaessin. 1996. Dacapo, a cyclin-dependent kinase inhibitor, stops cell proliferation during *Drosophila* development. *Cell.* 87:1225–1235.

Levanon, D., V. Negreanu, Y. Bernstein, I. Bar-Am, L. Avivi, and Y. Groner. 1994. AML1, AML2, and AML3, the human members of the runt domain gene-family: cDNA structure, expression, and chromosomal localization. *Genomics.* 23:425–432.

Li, Q.L., K. Ito, C. Sakakura, H. Fukamachi, K. Inoue, X.Z. Chi, K.Y. Lee, S. Nomura, C.W. Lee, S.B. Han, et al. 2002. Causal relationship between the loss of RUNX3 expression and gastric cancer. *Cell.* 109:113–124.

Lund, A.H., and M. van Lohuizen. 2002. RUNX: a trilogy of cancer genes. *Cancer Cell.* 1:213–215.

Morgenstern, J.P., and H. Land. 1990. A series of mammalian expression vectors and characterisation of their expression of a reporter gene in stably and transiently transfected cells. *Nucleic Acids Res.* 18:1068.

Mundlos, S., F. Otto, C. Mundlos, J.B. Mulliken, A.S. Aylsworth, S. Albright, D. Lindhout, W.G. Cole, W. Henn, J.H. Knoll, et al. 1997. Mutations involving the transcription factor CBFA1 cause cleidocranial dysplasia. *Cell.* 89:773–779.

Nakayama, K., N. Ishida, M. Shirane, A. Inomata, T. Inoue, N. Shishido, I. Horii, and D.Y. Loh. 1996. Mice lacking p27(^{KIP1}) display increased body size, multiple organ hyperplasia, retinal dysplasia, and pituitary tumors. *Cell.* 85:707–720.

Ogasawara, T., H. Kawaguchi, S. Jinno, K. Hoshi, K. Itaka, T. Takato, K. Nakamura, and H. Okayama. 2004. Bone morphogenetic protein 2-induced osteoblast differentiation requires Smad-mediated down-regulation of Cdk6. *Mol. Cell. Biol.* 24:6560–6568.

Ogawa, E., M. Maruyama, H. Kagoshima, M. Inuzuka, J. Lu, M. Satake, K. Shigesada, and Y. Ito. 1993. PEBP2/PEA2 represents a family of transcription factors homologous to the products of the *Drosophila* runt gene and the human AML1 gene. *Proc. Natl. Acad. Sci. USA.* 90:6859–6863.

Okahashi, N., Y. Murase, T. Koseki, T. Sato, K. Yamato, and T. Nishihara. 2001. Osteoclast differentiation is associated with transient upregulation of cyclin-dependent kinase inhibitors p21(WAF1/CIP1) and p27(KIP1). *J. Cell. Biochem.* 80:339–345.

Otto, F., A.P. Thornell, T. Crompton, A. Denzel, K.C. Gilmour, I.R. Rosewell, G.W. Stamp, R.S. Beddington, S. Mundlos, B.R. Olsen, et al. 1997. Cbfa1, a candidate gene for cleidocranial dysplasia syndrome, is essential for osteoblast differentiation and bone development. *Cell.* 89:765–771.

Pear, W.S., G.P. Nolan, M.L. Scott, and D. Baltimore. 1993. Production of high-titer helper-free retroviruses by transient transfection. *Proc. Natl. Acad. Sci. USA.* 90:8392–8396.

Perry, C., A. Eldor, and H. Soreq. 2002. Runx1/AML1 in leukemia: disrupted association with diverse protein partners. *Leuk. Res.* 26:221–228.

Philipp-Staheli, J., K.H. Kim, D. Liggitt, K.E. Gurley, G. Longton, and C.J. Kemp. 2004. Distinct roles for p53, p27Kip1, and p21Cip1 during tumor development. *Oncogene.* 23:905–913.

Pollack, J.R. 2002. RNA common reference sets. *In* DNA Microarrays: A Molecular Cloning Manual. D.D.L. Bowtell and J. Sambrook, editors. Cold Spring Harbor Laboratory, Cold Spring Harbor, NY. 168–177

Ponce-Castaneda, M.V., M.H. Lee, E. Latres, K. Polyak, L. Lacombe, K. Montgomery, S. Mathew, K. Krauter, J. Sheinfeld, J. Massague, et al. 1995. p27Kip1: chromosomal mapping to 12p12-12p13.1 and absence of mutations in human tumors. *Cancer Res.* 55:1211–1214.

Pratap, J., M. Galindo, S.K. Zaidi, D. Vradii, B.M. Bhat, J.A. Robinson, J.Y. Choi, T. Komori, J.L. Stein, J.B. Lian, et al. 2003. Cell growth regulatory role of Runx2 during proliferative expansion of preosteoblasts. *Cancer Res.* 63:5357–5362.

Sellers, W.R., B.G. Novitch, S. Miyake, A. Heith, G.A. Otterson, F.J. Kaye, A.B. Lassar, and W.G. Kaelin Jr. 1998. Stable binding to E2F is not required for the retinoblastoma protein to activate transcription, promote differentiation, and suppress tumor cell growth. *Genes Dev.* 12:95–106.

Serrano, M., A.W. Lin, M.E. McCurrach, D. Beach, and S.W. Lowe. 1997. Oncogenic ras provokes premature cell senescence associated with accumulation of p53 and p16INK4a. *Cell.* 88:593–602.

Sherr, C.J., and J.M. Roberts. 1999. CDK inhibitors: positive and negative regulators of G1-phase progression. *Genes Dev.* 13:1501–1512.

Sims, N.A., P. Clement-Lacroix, F. Da Ponte, Y. Bouali, N. Binart, R. Moriggl, V. Goffin, K. Coschigano, M. Gaillard-Kelly, J. Kopchick, et al. 2000. Bone homeostasis in growth hormone receptor-null mice is restored by IGF-I but independent of Stat5. *J. Clin. Invest.* 106:1095–1103.

Slingerland, J., and M. Pagano. 2000. Regulation of the cdk inhibitor p27 and its deregulation in cancer. *J. Cell. Physiol.* 183:10–17.

Stein, G.S., J.B. Lian, J.L. Stein, A.J. van Wijnen, and M. Monetcino. 1996. Transcriptional control of osteoblast growth and differentiation. *Physiol. Rev.* 76:593–629.

Sunters, A., D.P. Thomas, W.A. Yeudall, and A.E. Grigoriadis. 2004. Accelerated cell cycle progression in osteoblasts overexpressing the c-*fos* proto-oncogene: induction of cyclin A and enhanced CDK2 activity. *J. Biol. Chem.* 279:9882–9891.

Thirunavukkarasu, K., M. Mahajan, K.W. McLarren, S. Stifani, and G. Karsenty. 1998. Two domains unique to osteoblast-specific transcription factor Osf2/Cbfa1 contribute to its transactivation function and its inability to heterodimerize with Cbfbeta. *Mol. Cell. Biol.* 18:4197–4208.

Thomas, D.M., S.A. Carty, D.M. Piscopo, J.S. Lee, W.F. Wang, W.C. Forrester, and P.W. Hinds. 2001. The retinoblastoma protein acts as a transcriptional coactivator required for osteogenic differentiation. *Mol. Cell.* 8:303–316.

Toguchida, J., K. Ishizaki, M.S. Sasaki, Y. Nakamura, M. Ikenaga, M. Kato, M. Sugimot, Y. Kotoura, and T. Yamamuro. 1989. Preferential mutation of paternally derived RB gene as the initial event in sporadic osteosarcoma. *Nature.* 338:156–158.

Tsuji, K., Y. Ito, and M. Noda. 1998. Expression of the PEBP2αA/AML3/CBFA1 gene is regulated by BMP4/7 heterodimer and its overexpression suppresses type I collagen and osteocalcin gene expression in osteoblastic and nonosteoblastic mesenchymal cells. *Bone.* 22:87–92.

Yang, Y.H., S. Dudoit, P. Luu, D.M. Lin, V. Peng, J. Ngai, and T.P. Speed. 2002. Normalization for cDNA microarray data: a robust composite method addressing single and multiple slide systematic variation. *Nucleic Acids Res.* 30:e15.